

MAGNETIC PHASE TRANSITION IN TbMn_2Ge_2

J. Leciejewicz

Institute of Nuclear Chemistry and Technology, Warszawa, Poland

and

A. Szytuła

Institute of Physics, Jagiellonian University, Kraków, Poland

(Received 8 September 1983 by E.F. Bertaut)

The crystal and magnetic structure of TbMn_2Ge_2 are determined by neutron diffraction using a powder sample. The crystal structure of this compound is of the ThCr_2Si_2 type with small mixing of Mn and Ge atoms between 4(d) and 4(e) positions. At RT the antiferromagnetic collinear structure consists of $a + - + -$ sequence of ferromagnetic layers of Mn atoms with the magnetic moment parallel to the *c*-axis. At 85 K, the ferromagnetic ordering within the Tb sublattice is observed. The magnetic moment ($\sim 7.7 \mu_B$) is parallel to the *c*-axis. At 4.2 K additional reflections are observed, which correspond to antiferromagnetic components in a monoclinic unit cell.

1. INTRODUCTION

THIS REPORT IS A PART of a systematic study on magnetic structures of the ThCr_2Si_2 -type rare earth intermetallics, carried out by neutron diffraction method. So far we have reported the results on CeMn_2Si_2 [1], PrMn_2Si_2 and NdMn_2Si_2 [2], ErMn_2Si_2 and ErMn_2Ge_2 [3].

REMn_2X_2 compounds (where $X = \text{Si}$ and Ge) crystallize in the body-centred tetragonal structure of ThCr_2Si_2 -type (space group $I4/mmm$) [4]. The RE, Mn and Si or Ge atoms occupy the 2(a), 4(d) and 4(e) positions, respectively.

Magnetic measurements show that REMn_2X_2 compounds are either ferromagnets or antiferromagnets [5–7]. Polycrystalline sample of TbMn_2Ge_2 , however, shows ferromagnetic ordering at low temperature, attributed to the RE sublattice ($T_c = 33 \text{ K}$, $\mu = 6.02 \mu_B$ at 4.2 K and $H = 20 \text{ kOe}$) [5] and antiferromagnetic ordering connected with Mn sublattice at high temperatures ($T_N = 413 \text{ K}$) [7]. According to the magnetic data obtained on a single crystal the magnetization axis is parallel to the *c*-axis [8]. The magnetocrystalline anisotropy was found to be very large ($\sim 10^8 \text{ erg cm}^{-3}$) [8]. The saturation magnetic moment is $5.6 \mu_B$ i.e. smaller than the theoretical value expected for the free Tb^{3+} ion.

Neutron diffraction measurements were thus carried out made on polycrystalline TbMn_2Ge_2 sample. They gave surprising results, which are reported below.

2. EXPERIMENTAL AND RESULTS

The samples of TbMn_2Ge_2 were prepared by induction melting and solid state diffusion techniques.

X-ray analysis indicates that the sample has tetragonal structure of ThCr_2Si_2 -type.

Neutron diffraction measurements were performed at the EWA reactor at the former Institute of Nuclear Research in Świerk. Neutron diffraction data ($\lambda = 1.326 \times 10^{-1} \text{ nm}$) were collected by means of the DN-500 diffractometer at 293, 85 and 4.2 K (see Fig. 1). Additionally, the temperature dependence of magnetic peak heights was measured in the temperature range 4.2–293 K. The observed neutron intensities were treated with the line profile analysis method of Rietveld. Nuclear scattering lengths $b_{\text{Tb}} = 0.76$, $b_{\text{Mn}} = -0.39$ and $b_{\text{Ge}} = 0.819 \times 10^{-14} \text{ m}$ [9] were used. The magnetic form factor for Tb^{3+} ion was taken after [10].

Room temperature diffractogram of TbMn_2Ge_2 consists of strong reflections, satisfying the condition $h + k + l = 2n$, plus two superlattice lines, indexed as $M1\bar{1}1$ and $M1\bar{1}3$.

The nuclear intensities were calculated using the following atomic positions:

Tb atoms in the positions 2(a): $0, 0, 0, \frac{1}{2}, \frac{1}{2}, \frac{1}{2}$

in 4(d): $\frac{1}{2}, 0, \frac{1}{4}, 0, \frac{1}{2}, \frac{1}{4}, \frac{1}{2}, 0, \frac{3}{4}, 0, \frac{1}{2}, \frac{3}{4}$ $(1-e)\text{Mn} + e\text{Ge}$

in 4(e): $0, 0, z, 0, 0, \bar{z}, \frac{1}{2}, \frac{1}{2}, \frac{1}{2} + z, \frac{1}{2}, \frac{1}{2}, \frac{1}{2} - z$
 $(1-e)\text{Ge} + e\text{Mn}$

Table 1. Structural and magnetic parameters in TbMn_2Ge_2

| T (K) | 293 K | 85 K | 4.2 K |
|---------------------------------|------------|------------|------------|
| a (Å) | 4.006(2) | 4.006(4) | 3.972(3) |
| c (Å) | 10.875(6) | 10.842(8) | 10.758(8) |
| c/a | 2.715 | 2.706 | 2.708 |
| V (Å ³) | 174.52(27) | 174.00(47) | 169.73(44) |
| z | 0.3739(13) | 0.3744(14) | 0.3797(18) |
| μ_{Mn} (μ_B) | 2.1(2) | 2.3(2) | 2.3(3) |
| μ_{Tb}^F (μ_B) | — | 7.8(3) | 7.6(3) |
| R_N (%) | 4.3 | 4.5 | 4.9 |
| R_M (%) | 6.7 | 7.8 | 7.8 |

The minimum disagreement factor corresponded to the small mixing of Mn and Ge atoms between 4(d) and 4(e) positions ($e = 0.02$). The refined values of cell constant and z parameter and corresponding minimum R factor are listed in Table 1.

The observed superlattice $M1\bar{1}1$ and $M11\bar{3}$ lines are of magnetic origin. Similar magnetic reflections have been observed earlier in $\text{RE}\text{Mn}_2\text{Si}_2$ (RE = Ce, Pr and Nd Nd), YMn_2Ge_2 [1, 2] and ThMn_2Ge_2 [11]. Thus a collinear antiferromagnetic ordering whose ferromagnetic layers composed of the Mn atoms make $+-+$ sequence along the c -axis can be deduced persisting down to 4.2 K.

An increase of intensity of (101) , (110) and (103) peaks is observed on neutron diffraction pattern taken at 85 K, indicating the presence of a ferromagnetic ordering. The intensities analysis proved that parallel to the c -axis magnetic moments are localized on Tb atoms.

LHT neutron diffraction pattern contains additional reflections which were indexed on a monoclinic unit (m) cell obtained from the chemical one by the following transformation:

$$a_m = 2a_t, \quad b_m = a_t + c_t, \quad c_m = a_t.$$

Its dimensions are thus:

$$a_m = 7.944 \text{ \AA}, \quad b_m = 11.468 \text{ \AA}', \quad c_m = 3.972 \text{ \AA},$$

$$\gamma = 69.73^\circ.$$

This unit cell is displayed in Fig. 1. Tb ions occupy the positions:

$$S_1(0,0,0), \quad S_2(\frac{1}{2},0,0), \quad S_3(\frac{1}{2},\frac{1}{2},\frac{1}{2}), \quad S_4(0,\frac{1}{2},\frac{1}{2}),$$

Group theory analysis [12] shows that in this magnet magnetic unit cell, the only magnetic modes are the components of the following vectors:

$$F = S_1 + S_2 + S_3 + S_4, \quad G = S_1 - S_2 + S_3 - S_4.$$

$$C = S_1 + S_2 - S_3 - S_4, \quad A = S_1 - S_2 - S_3 + S_4.$$

F mode is ferromagnetic, while the other are

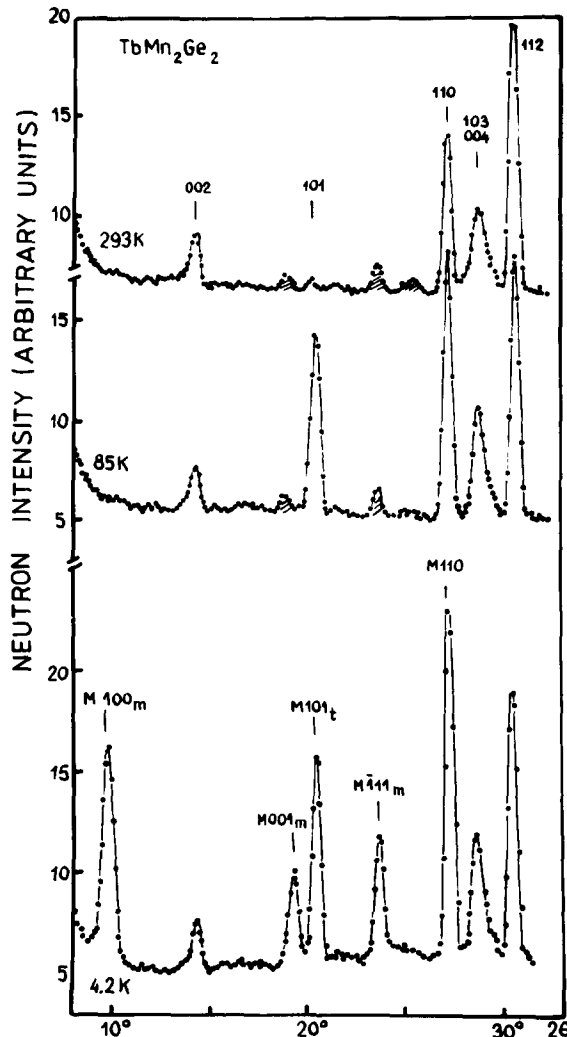
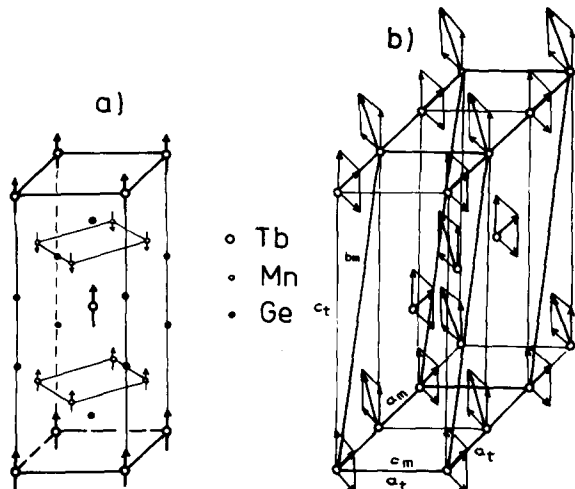


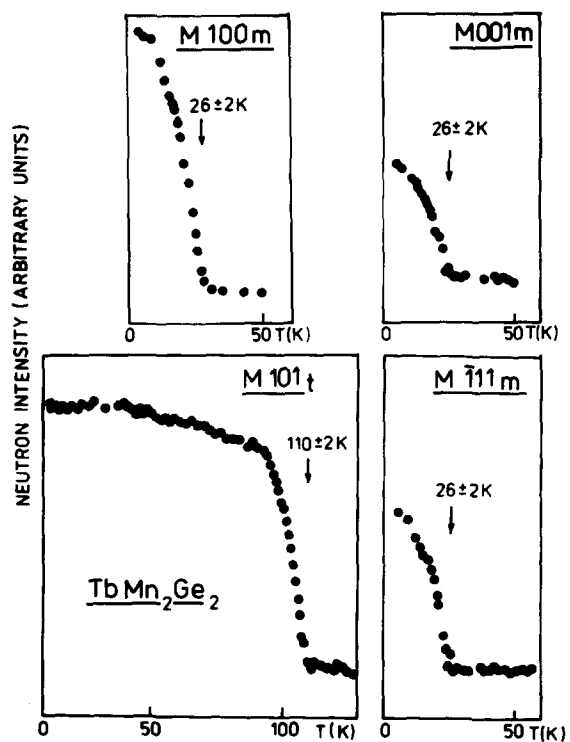
Fig. 1. Neutron diffraction patterns of TbMn_2Ge_2 at 4.2, 85 and 293 K. The reflections at 85 and 293 K are indexed in the tetragonal unit cell. The additional reflections at 4.2 K are indexed in the monoclinic unit cell (see Text). The shaded peaks arise from impurities. antiferromagnetic. The additional reflections observed at 4.2 K are allowed only in the A magnetic mode.

Table 2. Bragg angles $2\theta_B$ and magnetic intensities I at $T = 4.2$ K for TbMn_2Ge_2

| $h k l$ | $2\theta_B^{\text{obs}}$ | $2\theta_B^{\text{calc}}$ | I_{obs} | I_{calc} |
|------------------------------|--------------------------|---------------------------|------------------|-------------------|
| Antiferromagnetic components | | | | |
| 1 0 0 | 9.9 | 10.0 | 2921.4 | 2951.0 |
| 1 2 0 | — | 14.4 | — | 0 |
| 0 0 1 | 19.3 | 19.2 | 1185.7 | 1242.9 |
| 1 2 0 | 20.2 | 20.3 | 269.3 | 371.3 |
| 1 1 1 | 21.8 | — | 0 | 178.7 |
| 1 1 1 | 23.8 | 24.0 | 1455.65 | 1038.3 |
| 0 2 1 | | 24.0 | | 144.2 |
| 1 3 1 | — | 28.1 | 0 | 53.3 |
| 3 2 0 | — | 29.2 | 0 | 15.7 |
| R (%) | | | | 9.2 |
| Ferromagnetic components | | | | |
| 0 2 0 | — | 14.4 | — | 0 |
| 2 2 0 | | 20.5 | | 532.5 |
| 0 1 1 | 20.5 | 20.5 | 2942.9 | 815.5 |
| 2 0 0 | | 20.5 | | 1621.7 |
| 2 1 1 | 27.3 | 27.3 | 960.0 | 951.5 |
| 2 4 0 | | 29.0 | | 449.4 |
| 2 2 0 | 28.8 | 29.0 | 300.0 | 148.0 |
| R (%) | | | | 7.9 |

Fig. 2. Magnetic structure of TbMn_2Ge_2 : (a) tetragonal unit cell with the Tb and Mn sublattices at 85 K, (b) monoclinic unit cell with Tb sublattice at 4.2 K.

Their intensity analysis indicates, that the magnetic moment is parallel to the [1 2 0] direction. Its magnitude obtained in the course of least squares fit of observed and calculated integrated intensity amounts of 5.5 ± 0.1 Bohr magnetons. The A-mode can be presented as a sequence of ferromagnetic (0 1 0) planes coupled antiferromagnetically.

Fig. 3. Temperature dependence of height peaks of $M100_m$, $M001_m$, $M111_m$ and $M101_t$ reflections.

The reflections corresponding to ferromagnetic component are also indexed in the monoclinic unit cell (see Fig. 1 and Table 2). The best fit of observed and calculated intensity amounts to 7.6 ± 0.3 Bohr magnetons.

The total moment is however $9.1 \pm 0.3 \mu_B$ i.e. almost free ion value for Tb^{3+} ions.

Figure 3 shows the temperature vs. peak height curves of $(M1\ 0\ 0)_m$, $(M0\ 0\ 1)_m$, $(M\bar{1}\ 1\ 1)_m$ and $(M1\ 0\ 1)_t$ reflections. Accordingly the monoclinic antiferromagnetic structure transforms at 26 ± 2 K into a tetragonal ferromagnetic structure which is stable up to the Curie point at 110 ± 2 K.

3. SUMMARY

Our results indicate an interesting magnetic behaviour of TbMn_2Ge_2 :

(1) In the temperature range between 4.2 K and $T_N = 413$ K magnetic moments localized on Mn ions are ordered antiferromagnetically. The collinear magnetic structure consists of ferromagnetic layers stacked along the c -axis of a tetragonal unit cell with the sequence $+ - + -$. Moments are pointing along the c -axis.

(2) Below $T_c = 110$ K collinear ferromagnetic ordering of Tb moments along the c -axis is observed.

(3) At $T_t = 26$ K terbium magnetic sublattice transforms into an antiferromagnetic one. Magnetic moments have two components:

(a) ferromagnetic, which is parallel to the c -axis of a tetragonal unit cell, and

(b) antiferromagnetic, parallel to the $[1\ 2\ 0]$ direction in monoclinic unit cell.

Finally it is interesting to mention that TbMn_2Si_2 exhibits a complex, helicoidal type magnetic ordering of Tb moments persisting up to 56 K, apart from collinear antiferromagnetic order of Mn moments of $+ - + -$ type, stable up to 501 K [13].

REFERENCES

1. S. Siek, A. Szytuła & J. Leciejewicz, *Phys. Status Solidi (a)* **46**, K101 (1978).
2. S. Siek, A. Szytuła & J. Leciejewicz, *Solid State Commun.* **39**, 863 (1981).
3. J. Leciejewicz, S. Siek & A. Szytuła (unpublished).
4. Z. Ban & M. Sikirica, *Acta Cryst.* **18**, 594 (1965).
5. K.S.V.L. Narasimhan, V.U.S. Rao, R.L. Bergner & W.E. Wallace, *J. Appl. Phys.* **44**, 4597 (1976).
6. K.S.V.L. Narasimhan, V.U.S. Rao, W.E. Wallace & I. Pop, *AIP Conf. Proc.* **29**, 594 (1975).
7. A. Szytuła & I. Szott, *Solid State Commun.* **40**, 199 (1981).
8. T. Shigeoka, H. Fujii, H. Fujiwara, K. Yagasaki & T. Okamoto, *J. Magn. Magn. Mater.* **31-34**, 209 (1983).
9. G.E. Bacon, *Acta Cryst.* **A28**, 357 (1972).
10. O. Steinsvoll, C. Shirane, R. Nathans, M. Blume, H. Alperin & S.J. Pickart, *Phys. Rev.* **161**, 1499 (1967).
11. Z. Ban, L. Omejec, A. Szytuła & Z. Tomkowicz, *Phys. Status Solidi (a)* **27**, 333 (1973).
12. E.F. Bertaut, *Acta Cryst.* **A24**, 217 (1968).
13. S. Siek, A. Szytuła & J. Leciejewicz (unpublished).